

An Effective Data Augmentation for Person Re-identification

Yunpeng Gong, Zhiyong Zeng

College of Mathematics and Information, Fujian Normal University
{fmonkey625}@gmail.com, {zzyong}@fjnu.edu.cn

Abstract. In order to make full use of structural information of grayscale images and reduce adverse impact of illumination variation for person re-identification (ReID), an effective data augmentation method is proposed in this paper, which includes Random Grayscale Transformation, Random Grayscale Patch Replacement and their combination. It is discovered that structural information has a significant effect on the ReID model performance, and it is very important complementary to RGB images ReID. During ReID model training, on the one hand, we randomly selected a rectangular area in the RGB image and replace its color with the same rectangular area grayscale in corresponding grayscale image, thus we generate a training image with different grayscale areas; On the other hand, we convert an image into a grayscale image. These two methods will reduce the risk of overfitting the model due to illumination variations and make the model more robust to cross-camera. The experimental results show that our method achieves a performance improvement of up to 3.3%, achieving the highest retrieval accuracy currently on multiple datasets. The code is available at <https://github.com/finger-monkey/Data-Augmentation>.

Keywords: Person Re-identification, Data Augmentation, Random Grayscale Transformation, Random Grayscale Patch Replacement, Deep Learning.

1 Introduction

Person Re-identification (ReID) is usually viewed as an image retrieval matter, which aims to perform cross-camera retrieval of pedestrians to determine whether a particular pedestrian shows up in the image or video sequence taken by a camera. This is a challenging problem because images captured by different cameras often contain significant intra-class variations caused by variations of pedestrian posture, lighting, occlusion and so on, which lead to a significant reduction in the generalization ability of the ReID model. Hence, it is one of the major targets in ReID is to find some methods to effectively minimize the disadvantage of illumination variations.

For occlusion, Zhong et al proposed the Random Erasing [3] to simulate occlusion problems encountered in reality, which overcame the adverse impact of occlusion. As shown in the right picture of Fig.1.

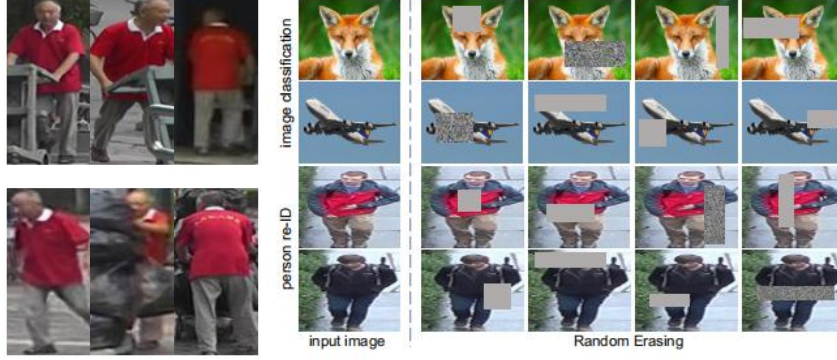


Fig. 1. The left figure is from the market1501[13] dataset and shows the main challenges faced by ReID such as perspective, body pose, light variation, and occlusion. The right figure shows the Random Erasing schematic.

ReID research articles published in recent years show that the generalization ability of ReID models is closely related to the training method of the models. For example, Luo, Liao et al. use many training tricks to effectively improve the performance of the model [1]. Liao proposed fastReID which used more training tricks [2], this method surpassed the highest performance of CVPR2020 model [4].

Fig.2 shows that images are most susceptible to lighting changes and lose more color information in environments of pedestrians replacing clothes and low resolution, but they have the same spatial structure. This variety is common in many datasets. A grayscale image is an RGB image which loses some color information but retains its spatial structure. In human cognition, humans can recognize different objects through grayscale images. Therefore, it is an important issue how to use spatial structural information to reduce the adverse impact of illumination changes on ReID.

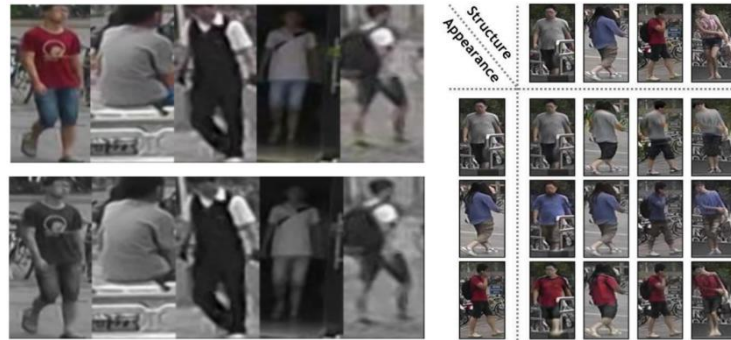


Fig. 2. Left: The first line are RGB images, the second line are the corresponding grayscale images. The images from left to right are: normal images with sharp contrast, low contrast dress, dark and gray dress, and blurred or low resolution images due to the movement of pedestrians(the images in the dataset are themselves of lower resolution). Right: Images of a pedestrian in different dresses, generated by GAN.

To show the importance of grayscale information for ReID query task, we designed the following experiments: dataset A1 is composed of RGB images, dataset A2 is composed of homogeneous grayscale images which is transformed by RGB images, A1 and A2 are trained and tested on the same model respectively, the ratio of the corresponding performance of the model on A1 and A2 is regarded as the contribution rate of grayscale information, as shown in Fig.3.

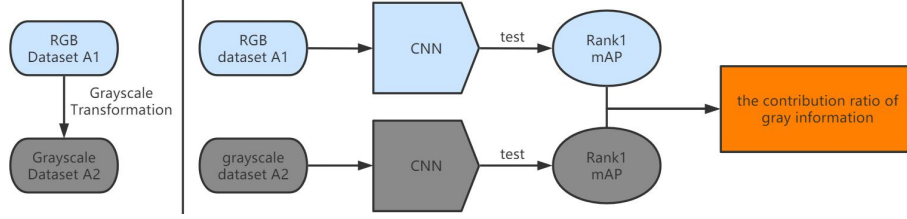


Fig. 3. The illustration is a schematic diagram of the experiment on the grayscale contribution.

Tested on three datasets, the contribution of grayscale images is shown in Tab.1.

Table 1. Contribution rate of grayscale information on MSMT17, DukeMTMC, and Market-1501 for the ReID.

Dataset	Rank-1	Rank-5	Rank-10	mAP
Market1501[13]	89.3%	95.4%	97.5%	73.4%
DukeMTMC[14]	91.0%	94.1%	95.2%	77.7%
MSMT17[16]	87.1%	91.7%	99.8%	70.6%

The experimental results show that grayscale images contribute more than 80% - 90% to the retrieval accuracy. More importantly, the contribution of grayscale images to the retrieval accuracy in Rank-10 is more than 95%. This result indicates that the spatial structure information of grayscale images has great potential for the ReID retrieval. Meanwhile, Zheng et al. used the generative adversarial network to change the clothes color of pedestrian in the image and generate more diverse data. This trick improves the ReID model's generalization ability [8], as is shown in the right column of Fig.2. Inspired by Zheng, we assume that homogeneous grayscale images of RGB images can also achieve the same goal of improving model performance, and can effectively reduce the impact of color variation produced by low contrast, the blurred images or low resolution images resulting from the movement of the pedestrians or changes in lighting.

Based on the above analysis, we propose a grayscale data augmentation method to improve the model performance. Grayscale Data Augmentation has the following advantages:

(1) It is a lightweight approach which does not require any additional parameter learning or memory consumption. It can be combined with various CNN models without changing the learning strategy.

(2) It is a complementary approach to existing data augmentation. When these methods are used altogether, Grayscale Data Augmentation can further improve model performance.

Our **main contributions** are summarized as follows:

(1) An effective grayscale data augmentation method is proposed to make full use of the structural information of grayscale images, which effectively minimizes adverse impact of illumination variation.

(2) We have conducted a large number of experiments on three ReID datasets and analyzed the experimental results, which demonstrates effectiveness of the proposed method.

The content of the remainder of the paper is as follows: Section 2 presents the related work, Section 3 presents the related algorithms, Section 4 presents the experimental results and analysis, and Section 5 presents a conclusion.

2 Related Work

Since deep learning was introduced into ReID field, many ReID methods have been proposed. An active field in ReID research is to utilize GANs to augment training data. For example, Zheng et al. used generative adversarial networks to replace the clothing of each pedestrian with the clothes of other pedestrians, so as to generate more diversified data to reduce the dependence of the model on color information and improve the generalization ability of the model [8]. In addition, some recent studies also employ some effective training tricks to improve the generalization ability of the model. For example, Luo et al. evaluate these effective training tricks in [1]. It's well known that data augmentation such as Random Cropping and Random Flipping plays an important role in the field of classification, detection and ReID, all of them increase the diversity of training data, and improve the generalization ability of the model to some extent. The Random Erasing proposed by Zhong et al. [3] simulates the occlusion problem that is frequently encountered in reality, which randomly erases a part of the image with a certain probability in the training samples to increase the diversity of the training samples. To some extent, it resolves the problems of inadequate generalization ability when the recognition task faces the occlusion problem, so it has become an effective training trick in the field of ReID. Fan et al. found that the learning rate has a great impact on the performance of a ReID model, a warmup strategy used is applied to bootstrap the network for better performance [5]. Label smoothing proposed is a widely used method to prevent overfitting for a classification task [6]. The k-reciprocal encoding is used to reorder the results of the query to improve mAP and Rank-1 [7]. This trick is known as re-Rank. The homogeneity of softmax loss and triplet loss functions was pointed out by Circle Loss, and a new loss to unify these two paradigms is proposed, the best ReID performance is achieved on Market-1501 dataset [15].

Furthermore, the VI-ReID[12] was proposed by Ye et al. In this method, grayscale images are only a bridge between visible images and infrared images. The

target of the proposed method is to show the effectiveness of grayscale data augmentation in cross-modal ReID.

3 The Proposed Approach

Given the fact that the structural information of grayscale images has a great impact on the performance of ReID, in order to take full advantage of the grayscale structural information and fit the color of RGB images, we propose an effective ReID data augmentation method in this paper: Grayscale Data Augmentation, which includes Random Grayscale Transformation(RGT), Random Grayscale Patch Replacement (RGPR), and their combination. The framework of the proposed method is shown in Fig.4 and Fig.5.

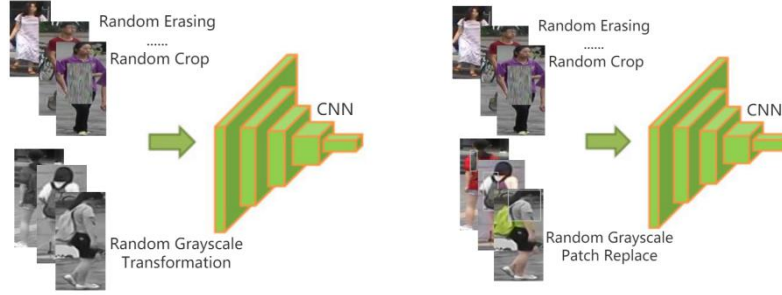


Fig. 4. Application of RGT(left) and RGPR(right) in pipelines of the baseline.



Fig. 5. Schematic diagram of Random Grayscale Patch Replacement.

3.1 Random Grayscale Transformation (RGT)

In order to diversify the data and preserve the spatial structure information of the RGB images, before training samples are input into neural network, we conduct RGT randomly transformation on the entire batch of training images with a certain probability. A grayscale image is generated by performing a pixel-by-pixel linear cumulative transformation on the R, G, B channels of the original RGB image. The procedure of RGT is shown in algorithm1.

Algorithm1 : Random Grayscale Transformation Procedure

Input : Input batch RGB images I ;
Gray transformation probability p ;
Output: mini-batch of grayscale images I^* .
1 Initialization: $p_1 \leftarrow \text{Rand}(0, 1)$.
2 if $p_1 \geq p$ then
3 $I^* \leftarrow I$;
4 return I^* .
5 End

3.2 Random Grayscale Patch Replace (RGPR)

In the process of model training, we conduct RGPR randomly transformation on the entire batch of training images with a certain probability. For an image I in a mini-batch, denote the probability of it undergoing RGPR be p_r , and the probability of it being kept unchanged be $1-p_r$. In this process, it randomly selects a rectangular region in the image and replaces it with the pixels of the same rectangular region in the corresponding grayscale image. Thus, training images which include regions with different levels of grayscale are generated. Among them, s_l and s_h are the minimum and maximum values of the ratio of the image to the randomly generated rectangle area, and the S_e of the rectangle area limited between the minimum and maximum ratio is obtained by $S_e \leftarrow \text{Rand}(s_l, s_h) \times S$, r_e is a coefficient used to determine the shape of the rectangle. It is limited to the interval (r_1, r_2) . x_e and y_e are randomly generated by coordinates of the upper left corner of the rectangle. If the coordinates of the rectangle exceed the scope of the image, the area and position coordinates of the rectangle are re-determined. When a rectangle that meets the above requirements is found, the pixel values of the selected region are replaced by the corresponding rectangular region on the grayscale image converted from RGB image. The whole algorithm is similar to Random Erasing. The difference is that Random Erasing randomly assigns the pixels of the selected region, and it will introduce noise into the image, while our method is to use the values of corresponding grayscale patch to replace the pixel values of the selected region. As a result, training images which include regions with different levels of grayscale are generated, and the object structure is not damaged. The procedure of RGPR is shown in Algorithm.2.

Algorithm 2: Random Grayscale Patch Replace Procedure

Input: Input image I ;
Image size W and H ;
Area of image S ;
Erasing probability p_r ;
Erasing area ratio range s_l and s_h ;
Erasing aspect ratio range r_1 and r_2 .

Output: Grayscale erased image I^* .

```

1 Initialization:  $p_1 \leftarrow \text{Rand}(0, 1)$ .
2 if  $p_1 \geq p_r$  then
3    $I^* \leftarrow I$ ;
4   return  $I^*$  .
5 else
6   while True do
7      $S_e \leftarrow \text{Rand}(s_l, s_h) \times S$ ;
8      $r_e \leftarrow \text{Rand}(r_1, r_2)$ ;
9      $H_e \leftarrow \text{Sqrt}(S_e \times r_e)$ ,  $W_e \leftarrow \text{Sqrt}(S_e / r_e)$ ;
10     $x_e \leftarrow \text{Rand}(0, W)$ ,  $y_e \leftarrow \text{Rand}(0, H)$ ;
11    if  $x_e + W_e \leq W$  and  $y_e + H_e \leq H$  then
12       $I_e \leftarrow (x_e, y_e, x_e + W_e, y_e + H_e)$ ;
13       $I(I_e) \leftarrow \text{Grayscale}(I_e)$ ;
14       $I^* \leftarrow I$ ;
15      return  $I^*$ 
16    end
17 end
18
```

4 Comparison and Analysis

In this section we will compare the performance of our approach with state-of-the-art methods on three baselines. The baselines are the ReID_baseline[10], the strong baseline [1] and FastReID[2]. Since the model requires more training epochs to fit than the original, we add 0.5-1.5 times more training epochs to the training process.

4.1 Datasets

We conducted comparison experiments on MTMC17[16], DukeMTMC[14], and Market-1501[13].

The MSMT17 dataset, created in winter, was presented in 2018 as a new, larger dataset closer to real-life scenes, containing a total of 4,101 individuals and covering multiple scenes and time periods.

The DukeMTMC is a large-scale Multi-Target, Multi-Camera (MTMC) tracking dataset, a HD video dataset recorded by 8 synchronous cameras, with more than 7,000 single camera tracks and more than 2,700 individual pedestrians.

The Market-1501 dataset was collected in the summer of 2015. It includes 1,501 pedestrians captured by six cameras (five HD cameras and one low-definition camera).

These three datasets are currently the largest datasets of ReID, and they are also the most representative because they collectively contain multi-season, multi-time, HD, and low-definition cameras with rich scenes and backgrounds as well as complex lighting variations.

We evaluated these three datasets using Rank-k precision and mean Average Precision (mAP). Rank-1 denotes the average accuracy of the first returned result corresponding to each query image; mAP denotes the mean of average accuracy, the query results are sorted according to the similarity, the closer the correct result is to the top of the list, the higher the score.

4.2 Hyper-Parameter Setting

During CNN training, two hyper-parameters need to be evaluated. One of them is RGT probability p . Firstly, we take the hyper-parameter p as 0.01, 0.03, 0.05, 0.07, 0.1, 0.2, 0.3, ..., 1 for the RGT experiments. Then we take the value of each parameter for three independent repetitions of the experiments. Finally, we calculate the average of the final result. The results of different p are shown in Fig.6.

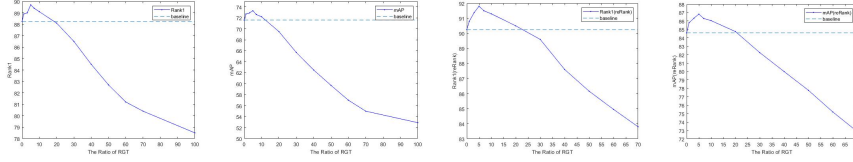


Fig. 6. Accuracy under different hyper-parameters on Market-1501 using baseline[10].

We can see that when $p=0.05$, the performance of the model reaches the maximum value in Rank-1 and mAP in Fig.7. If we do not specify, the hyper-parameter is set $p=0.05$ in the next experiments.

Another hyper-parameter is RGPR probability p_r . We take the hyper-parameter p_r as 0.01, 0.03, 0.05, 0.07, 0.1, 0.2, 0.3, ..., 1 for the RGPR experiments, whose selection process is similar to the above p . The results of different p_r are shown in Fig.7.

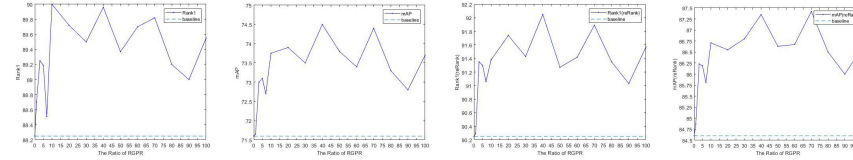


Fig. 7. Accuracy under different hyper-parameters on Market-1501 using baseline[10].

Obviously, when $p_r=0.4$ or $p_r=0.7$, the model achieves better performance. And the best performance is achieved when $p_r=0.4$. If we do not specify, the hyper-parameter is set $p_r=0.4$ in the later experiments.

4.3 Effectiveness of RGT and RGPR

Evaluation of RGT and RGPR. Compared with the best results of RGT on baseline [10], the accuracy of RGPR is improved by 0.5% and 1.4% on Rank-1 and mAP, respectively. Under the same conditions using re-Rank, the accuracy of Rank-1 and mAP is improved by 0% and 0.4%, respectively. Therefore, the advantages of RGPR are more obvious when re-Rank is not used. However, Fig.8 also shows that the performance improvement brought by RGPR is not stable enough because of the obvious fluctuation in RGPR, while the performance improvement brought by RGT is very stable. Therefore, we improve the stability of the method by combining RGT with RGPR.

Evaluation by Combining RGT with RGPR. First, we fix the hyper-parameter value of RGT to $p=0.05$, then keep the control variable unchanged to further determine the hyper-parameter of RGPR. Finally, we take the hyper-parameter p_r of RGPR to be 0.1, 0.2, \dots , 0.7 to conduct combination experiments of RGT and RGPR, and conduct 3 independent repeated experiments for each parameter p_r to get the average value. The result is shown in Fig.8:

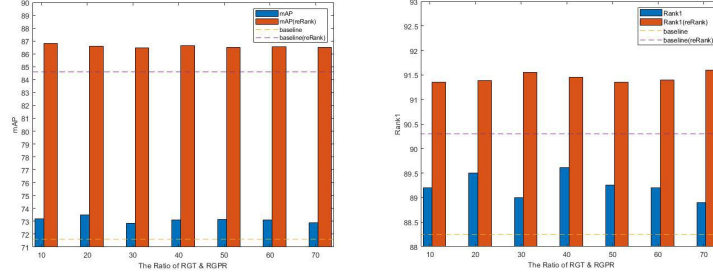


Fig. 8. Model performance of combining RGT with RGPR.

It can be seen from Fig.8 that the performance improvement brought by the combination of RGT and RGPR is more stable and with less fluctuation, and the comprehensive performance of the model is the best when the hyper-parameter value of RGPR is $p_r=0.4$.

4.4 Performance Comparison and Analysis

We first evaluate each baseline on the Market-1501 dataset. Our method improves by 1.2% on Rank-1 and 3.3% on mAP on ReID_baseline [10], and 1.5% on Rank-1 and 2.1% on mAP above baseline in the same conditions using the re-Rank. The best results of our method improve by 0.6% and 1.3% on the Rank-1 and mAP on

the strong baseline [1], respectively, and 0.8% and 0.5% Rank-1 and mAP above baseline under the same conditions using the re-Rank, respectively. On fastReID [2], our method is 0.2% higher and 0.9% than baseline in Rank-1 and mAP, respectively, and higher 0.1% and 0.3% than baseline under using re-Rank.

A comparison of the performance of our method with the state-of-the-art methods in three datasets is shown in Table 2 and Table 3.

Table 2. Performance comparison on MTMC17 datasets.

Methods	MTMC17	
	Rank-1	mAP
IANet[25] (CVPR’19)	75.5	46.8
DGNet[8](CVPR’19)	77.2	52.3
OSNet[9](ICCV’19)	78.7	52.9
BAT-net[11](ICCV’19)	79.5	56.8
RGA-SC[19](CVPR’20)	80.3	57.5
SCSN[18](CVPR’20)	83.8	58.5
AdaptiveReID[17](arXiv’20)	81.7	62.2
fastReID[2]	85.1	63.3
fastReID + RGT(ours)	86.2	65.3
fastReID + RGT&RGPR(ours)	86.2	65.9

Table 3. Performance comparison on DukeMTMC、Market-1501 datasets.

Methods	Market1501		DukeMTMC	
	Rank-1	mAP	Rank-1	mAP
PCB [20] (ECCV’18)	92.3	77.4	81.8	66.1
AANet [24] (CVPR’19)	93.9	83.4	87.7	74.3
IANet [25] (CVPR’19)	94.4	83.1	87.1	73.4
Auto-ReID [28] (ICCV’19)	94.5	85.1	—	—
DG-Net[8](CVPR’19)	94.8	86.0	86.6	74.8
Pyramid [26] (CVPR’19)	95.7	88.2	89.0	79.0
ABDNet [27] (ICCV’19)	95.6	88.3	89.0	78.6
SONA [22] (ICCV’19)	95.7	88.7	89.3	78.1
SCAL [23] (ICCV’19)	95.8	89.3	89.0	79.6
CAR [21] (ICCV’19)	96.1	84.7	86.3	73.1
Circle Loss [15] (CVPR’20)	96.1	87.4	89.0	79.6
ReID_baseline[10]	88.8	71.6	—	—
ReID_baseline + reRank	90.5	85.2	—	—
ReID_baseline + RGT(ours)	89.5	73.5	—	—
ReID_baseline + RGT+ reRank(ours)	92.0	86.9	—	—
ReID_baseline + RGPR(ours)	90.0	74.9	—	—
ReID_baseline + RGPR + reRank(ours)	92.0	87.4	—	—
strong baseline[1]	94.5	85.9	86.4	76.4
strong baseline + reRank	95.4	94.2	90.3	89.1
strong baseline + RGT(ours)	94.6	85.7	87.8	77.3
strong baseline + RGT + reRank(ours)	96.2	94.7	90.9	89.2

strong baseline + RGPR(ours)	95.1	87.2	87.3	77.3
strong baseline + RGPR + reRank(ours)	95.9	94.4	91	89.4
fastReID[2]	96.3	90.3	92.4	83.2
fastReID + reRank	96.8	95.3	94.4	92.2
fastReID + RGT(ours)	96.5	91.2	—	—
fastReID + RGT + reRank(ours)	96.9	95.6	—	—
fastReID + RGPR(ours)	—	—	92.8	84.2
fastReID + RGPR + reRank(ours)	—	—	94.3	92.7

Next we evaluate each baseline on DukeMTMC dataset, the best results of our method on the strong baseline [1] improved by 1.4% on Rank-1, 0.9% on mAP, respectively, and 0.7% on Rank-1, 0.3% on mAP using the re-Rank, respectively. Our method on fast-ReID[2] improves by 0.4% and 1% on Rank-1 and mAP, respectively, and higher 0.5% on mAP than baseline under using the re-Rank.

Finally, we evaluate each baseline on the MTMC17 dataset, the best results of our method on fastReID[2] improve by 1.1% and 2.6% over baseline on Rank-1 and mAP, respectively.

To our knowledge, applying our approach to fastReID, we have achieved the highest retrieval accuracy currently available on the MTMC17 and Market-1501 datasets.

On the one hand, our method achieves better ReID performance because of exploiting the grayscale transformation, which increases the number and diversity of training samples. On the other hand, exploiting the structural information retained by the grayscale image, the colors of the RGB images and the spatial structural information of the grayscale images are fitted to each other in the model training, reducing the adverse effects of illumination variations on ReID.

5 Conclusion

In this paper, we propose a simple and effective method called Grayscale Data Augmentation for ReID. Neither does the method require large scale training like GAN, nor introduces any noise. In addition, it can increase the diversity of training samples. Meanwhile, the method achieves diversity training samples using a simple homogeneous grayscale transformation and preserves the structural information of the original color images. RGB images and grayscale images with a certain probability are jointly input in the network during the training process, which is actually to train the network model using the color information and spatial structure information of the images, the spatial structure information of grayscale images is well fitted with the color information of color images, it will minimize the adverse impacts of illumination variations for ReID. The effectiveness of the proposed method is verified by experiments on multiple datasets and test benchmarks, and exceeds the performance of the currently optimal algorithm.

References

1. Hao Luo, Youzhi Gu, Xingyu Liao, Shenqi Lai, Wei Jiang; Bag of Tricks and A Strong Baseline for Deep Person Re-identification. In the IEEE Conference on Computer Vision and Pattern Recognition (CVPR) Workshops, 2019.
2. Lingxiao He, Xingyu Liao, Wu Liu, Xinchun Liu, Peng Cheng, Tao Mei; FastReID: A Pytorch Toolbox for General Instance Re-identification arXiv preprint arXiv :2006.02631,2020.
3. Zhun Zhong, Liang Zheng, Guoliang Kang, Shaozi Li, and Yi Yang. Random erasing data augmentation. arXiv preprint arXiv:1708.04896, 2017.
4. Yifan Sun, Changmao Cheng, Yuhua Zhang, Chi Zhang, Liang Zheng, Zhongdao Wang, Yichen Wei; Circle loss:A unified perspective of pair similarity optimization.The IEEE/CVF Conference on Computer Vision and Pattern Recognition (CVPR), 2020.
5. Xing Fan, Wei Jiang, Hao Luo, and Mengjuan Fei. SphereReID: Deep hypersphere manifold embedding for person re-identification. Journal of Visual Communication and Image Representation, 2019.
6. Christian Szegedy, Vincent Vanhoucke, Sergey Ioffe, Jon Shlens, and Zbigniew Wojna. Rethinking the inception architecture for computer vision. In Proceedings of the IEEE conference on computer vision and pattern recognition, pages 2818–2826, 2016.
7. Zhun Zhong, Liang Zheng, Donglin Cao, and Shaozi Li. Re-ranking person re-identification with k-reciprocal encoding. In The IEEE Conference on Computer Vision and Pattern Recognition (CVPR), 2017.
8. Zheng, Zhedong and Yang, Xiaodong and Yu, Zhiding and Zheng, Liang and Yang, Yi and Kautz, Jan; Joint Discriminative and Generative Learning for Person Re-identification. In the IEEE Conference on Computer Vision and Pattern Recognition (CVPR) 2019.
9. Kaiyang Zhou, Yongxin Yang, Andrea Cavallaro, and Tao Xiang. Omni-scale feature learning for person re-identification. In The IEEE International Conference on Computer Vision (ICCV), 2019.
10. https://github.com/layumi/ReID_baseline_pytorch
11. P. Fang, J. Zhou, S. K. Roy, L. Petersson, and M. Harandi. Bilinear attention networks for person retrieval. In The IEEE International Conference on Computer Vision (ICCV), 2019, pp. 8030–8039.
12. M. Ye, J. Shen and L. Shao, Visible-Infrared Person Re-Identification via Homogeneous Augmented Tri-Modal Learning, in IEEE Transactions on Information Forensics and Security, doi: 10.1109/TIFS.2020.3001665.
13. Liang Zheng, Liyue Shen, Lu Tian, Shengjin Wang, Jing-dong Wang, and Qi Tian. Scalable person re-identification: A benchmark. In ICCV, 2015.
14. Z. Zheng, L. Zheng, and Y. Yang. Unlabeled samples generated by gan improve the person re-identification baseline in vitro. In ICCV, 2017.
15. Yifan Sun, Changmao Cheng, Yuhua Zhang, Chi Zhang, Liang Zheng, Zhongdao Wang, and Yichen Wei. Circle loss: A unified perspective of pair similarity optimization. In the IEEE Conference on Computer Vision and Pattern Recognition (CVPR), 2020.
16. Longhui Wei, Shiliang Zhang, Wen Gao, Qi Tian; Person Transfer GAN to Bridge Domain Gap for Person Re-Identification Proceedings of the IEEE Conference on Computer Vision and Pattern Recognition (CVPR), 2018.
17. Xingyang Ni, Liang Fang, Heikki Huttunen. AdaptiveReID: Adaptive L2 Regularization in Person Re-Identification. arXiv preprint arXiv :2007.07875, 2020.

18. X. Chen, C. Fu, Y. Zhao, F. Zheng, J. Song, R. Ji, and Y. Yang. Saliency-Guided Cascaded Suppression Network for Person ReIdentification. In The IEEE Conference on Computer Vision and Pattern Recognition (CVPR), 2020.
19. Z. Zhang, C. Lan, W. Zeng, X. Jin, and Z. Chen. Relation-Aware Global Attention for Person Re-identification. In The IEEE Conference on Computer Vision and Pattern Recognition (CVPR), 2020.
20. Yifan Sun, Liang Zheng, Yi Yang, Qi Tian, and Shengjin Wang. Beyond part models: Person retrieval with refined part pooling (and a strong convolutional baseline). In The European Conference on Computer Vision (ECCV), 2018.
21. Kaiyang Zhou, Yongxin Yang, Andrea Cavallaro, and Tao Xiang. Omni-scale feature learning for person re-identification. In The IEEE International Conference on Computer Vision (ICCV), 2019.
22. Bryan (Ning) Xia, Yuan Gong, Yizhe Zhang, and Christian Poellabauer. Second-order non-local attention networks for person re-identification. In The IEEE International Conference on Computer Vision (ICCV), 2019.
23. Binghui Chen, Weihong Deng, and Jiani Hu. Mixed highorder attention network for person re-identification. In The IEEE International Conference on Computer Vision (ICCV), 2019.
24. Chiat-Pin Tay, Sharmili Roy, and Kim-Hui Yap. Aanet: Attribute attention network for person re-identifications. In The IEEE Conference on Computer Vision and Pattern Recognition (CVPR), 2019.
25. Ruibing Hou, Bingpeng Ma, Hong Chang, Xinqian Gu, Shiguang Shan, and Xilin Chen. Interaction-and-aggregation network for person re-identification. In The IEEE Conference on Computer Vision and Pattern Recognition (CVPR), 2019.
26. Feng Zheng, Cheng Deng, Xing Sun, Xinyang Jiang, Xiaowei Guo, Zongqiao Yu, Feiyue Huang, and Rongrong Ji. Pyramidal person re-identification via multi-loss dynamic training. In The IEEE Conference on Computer Vision and Pattern Recognition (CVPR), 2019.
27. Binghui Chen, Weihong Deng, and Jiani Hu. Mixed highorder attention network for person re-identification. In The IEEE International Conference on Computer Vision (ICCV), 2019.
28. Ruijie Quan, Xuanyi Dong, Yu Wu, Linchao Zhu, and Yi Yang. Auto-ReID: Searching for a part-aware convnet for person re-identification. In The IEEE International Conference on Computer Vision (ICCV), 2019.